www.iosrjournals.org

# **Title**

# Author

## Abstract:

**Background**: This study focuses on a natural convention flow of Silicon (IV)Oxide-water nanofluid in a magnetically equipped exponentially stretching surface in a three-dimensional frame. The effects of buoyancy, nanoparticle volume fractions and magnetism on the flow velocities in all directions, temperature of flow and concentration of the nanoparticles.

Material and methods: The study considered a steady boundary layer flow of an electrically conducting nanofluid past a semi-infinite convectively heated flat plate in the presence of a uniform transverse magnetic field. It assumed that the induced magnetic field and the external electric field were negligible. The governing equations were subject to the boundary conditions and were solved numerically by the Runge-Kutta-Fehlberg method with shooting technique. Both velocity and temperature profiles were obtained and utilized to compute the skin-friction coefficient and the local Nusselt number in the equation.

**Results:** The numerical simulations reveal that an increase in Grashof number (Gr) lead to an enhancement in both the primary (f') and secondary (g') velocity components. This was due to the buoyancy forces strengthening the convective transport of fluid and nanoparticles so that buoyancy forces became stronger as Gr increases, and consequently leading to an increase in the fluid velocity.

**Conclusion:** Grashof number and nanoparticle volume fraction enhances primary and secondary velocities, magnetic field reduces both primary and secondary velocities, nanoparticle volume fractions increase temperature profile, and nanoparticle volume fractions concentration of nanoparticles decreases.

**Key Words:** Nusselt number, Grashof number, Velocity components, Heat transfer, Thermal conductivity, nanoparticles, Magnetic field strength, Nanofluid.

Date of Submission: 01-11-2025

Date of Acceptance: 10-11-2025

Date of Submission. 01-11-2025

## I. Introduction

Fluids generally have poor thermal conductivity and are unable to handle thermal requirements for industrial processes such as in industrial cooling, and electronic thermal management. By dispersing some nanoparticles in the fluids, a suspension referred to as nanofluid is formed and the electrical and thermal properties of the fluid are improved. Studies on nanofluids revealed that nanofluids have the tendency to solve the thermal problems in industrial settings due to the superiority of their thermophysical properties compared to the base fluids.

By harnessing the thermal and electrical properties of the nanoparticles, the nanofluid formed from the colloidal suspension produces higher thermophysical properties that makes the nanofluid superior to the base fluids.

Equipping a flow with magnetic field produces an effect referred to as magnetohydrodynamic (MHD) effects. The effect becomes magnified when the fluid is carrying highly conductive and electrically sensitive components. Hence, the flow of thermally and electrically enhanced nanofluids under influence of magnetic force is expected to be influenced significantly.

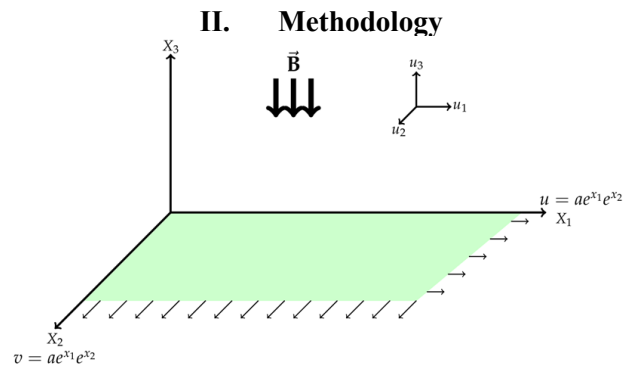


Figure. 1: Flow configuration

The flow configuration, as depicted in Figure 1, illustrates the system under consideration in this study. The flow is steady and occurs within a three-dimensional framework, where a magnetic field (MF) is applied along the vertical axis. The nanofluid flows within the  $x_1x_2$ -plane due to the influence of the MF, which is oriented at an angle of 90° to the flow plane.

# **Fundamental Equations**

## Continuity equation

letting  $\mathbf{u} = (u_1, u_2, u_3)$  be the velocity field,  $(x_1, x_2, x_3)$  the space coordinates  $\Rightarrow \frac{\partial u_1}{\partial x_1} + \frac{\partial u_2}{\partial x_2} + \frac{\partial u_3}{\partial x_3} = 0.$ 

$$\Rightarrow \frac{\partial u_1}{\partial x_1} + \frac{\partial u_2}{\partial x_2} + \frac{\partial u_3}{\partial x_3} = 0$$

## Momentum equations

The momentum equations, also commonly referred to as Navier-Stokes equations, are derived from the Newton's second law of motion.

The general momentum equation for incompressible steady Newtonian flow is

$$\sum_{j} u_{j} \frac{\partial u_{i}}{\partial x_{j}} = -\frac{1}{\rho} \frac{\partial p}{\partial x_{i}} + \frac{\mu}{\rho} \sum_{j} \frac{\partial^{2} u_{i}}{\partial x_{j}^{2}} + \frac{1}{\rho} f_{i}.$$

Thus, the momentum equations in the three directions are

$$\begin{split} u_1 \frac{\partial u_1}{\partial x_1} + u_2 \frac{\partial u_1}{\partial x_2} + u_3 \frac{\partial u_1}{\partial x_3} &= -\frac{1}{\rho} \frac{\partial p}{\partial x_1} + \frac{\mu}{\rho} \left( \frac{\partial^2 u_1}{\partial x_1^2} + \frac{\partial^2 u_1}{\partial x_2^2} + \frac{\partial^2 u_1}{\partial x_3^2} \right) + g\beta(T - T_{\infty}) - \frac{\sigma B_0^2}{\rho} u_1, \\ u_1 \frac{\partial u_2}{\partial x_1} + u_2 \frac{\partial u_2}{\partial x_2} + u_3 \frac{\partial u_2}{\partial x_3} &= -\frac{1}{\rho} \frac{\partial p}{\partial x_2} + \frac{\mu}{\rho} \left( \frac{\partial^2 u_2}{\partial x_1^2} + \frac{\partial^2 u_2}{\partial x_2^2} + \frac{\partial^2 u_2}{\partial x_3^2} \right) + g\beta(T - T_{\infty}) - \frac{\sigma B_0^2}{\rho} u_2, \\ u_1 \frac{\partial u_3}{\partial x_1} + u_2 \frac{\partial u_3}{\partial x_2} + u_3 \frac{\partial u_3}{\partial x_2} &= -\frac{1}{\rho} \frac{\partial p}{\partial x_3} + \frac{\mu}{\rho} \left( \frac{\partial^2 u_3}{\partial x_1^2} + \frac{\partial^2 u_3}{\partial x_2^2} + \frac{\partial^2 u_3}{\partial x_2^2} \right). \end{split}$$

The boundary layer analysis is used to reduce the complexity of the problem by leveraging the characteristic length scales and flow behaviour near the boundary. The assumptions of the boundary layer theory are as follows;

- 1. The boundary layer is very thin compared to the characteristic length L of the flow.
- 2. In the boundary layer, there is a strong variation in the velocity in the direction normal to the surface, but the variation along the surface is small.
- 3. The pressure is assumed to be constant in the direction tangential to the surface and can only vary in the direction normal to the surface.
- 4. Some terms are assumed to be negligible based on scaling arguments, which depend on the relative magnitude of different terms.

Now,  $x_1$  and  $x_2$  are the primary flow directions (tangential to the surface) and  $x_3$  is the direction normal to the surface. The boundary layer develops along  $x_1$  and  $x_2$ , while variations in  $x_3$  are much stronger within the thin boundary layer.

The order of magnitude for the viscous terms are as follows;

$$O\left(\frac{\partial^2 u_1}{\partial x_1^2}\right) = O\left(\frac{\partial^2 u_1}{\partial x_2^2}\right) = O\left(\frac{\partial^2 u_2}{\partial x_1^2}\right) = O\left(\frac{\partial^2 u_2}{\partial x_2^2}\right) = O\left(\frac{a}{L^2}\right), \quad \text{(negligible)}$$

$$O\left(\frac{\partial^2 u_1}{\partial x_3^2}\right) = O\left(\frac{\partial^2 u_2}{\partial x_3^2}\right) = O\left(\frac{a}{\delta^2}\right)$$

$$O\left(\frac{\partial^2 u_3}{\partial x_1^2}\right) = O\left(\frac{\partial^2 u_3}{\partial x_2^2}\right) = O\left(\frac{\delta a}{L^2}\right) = O\left(\frac{\delta a}{L^2}\right) \quad \text{(negligible)}$$

$$O\left(\frac{\partial^2 u_3}{\partial x_3^2}\right) = O\left(\frac{\frac{\delta}{L}a}{\delta^2}\right) = O\left(\frac{a}{\delta L}\right) \quad \text{(negligible)}$$

This implies that the terms

$$\frac{\partial^2 u_1}{\partial x_1^2}$$
,  $\frac{\partial^2 u_1}{\partial x_2^2}$ ,  $\frac{\partial^2 u_2}{\partial x_1^2}$ , and  $\frac{\partial^2 u_2}{\partial x_2^2}$ 

are small and can be ignored but the terms

$$\frac{\partial^2 u_1}{\partial x_3^2}$$
 and  $\frac{\partial^2 u_2}{\partial x_3^2}$ 

are large and must be retained. The order of magnitude for the pressure terms are as follows;

$$O\left(\frac{\partial p}{\partial x_1}\right) = O\left(\frac{\partial p}{\partial x_2}\right) = O\left(\frac{p}{L}\right), \ O\left(\frac{\partial p}{\partial x_3}\right) = O\left(\frac{p}{\delta}\right)$$

Removing terms of negligible order, the momentum equations are left with:

- The  $x_1$  momentum equation becomes

$$u_1 \frac{\partial u_1}{\partial x_1} + u_2 \frac{\partial u_1}{\partial x_2} + u_3 \frac{\partial u_1}{\partial x_3} = -\frac{1}{\rho} \frac{\partial p}{\partial x_1} + \frac{\mu}{\rho} \frac{\partial^2 u_1}{\partial x_1^2} + g\beta(T - T_{\infty}) - \frac{\sigma B_0^2}{\rho} u_1$$

- The  $x_2$  momentum equation becomes

$$u_1 \frac{\partial u_2}{\partial x_1} + u_2 \frac{\partial u_2}{\partial x_2} + u_3 \frac{\partial u_2}{\partial x_3} = -\frac{1}{\rho} \frac{\partial p}{\partial x_2} + \frac{\mu}{\rho} \frac{\partial^2 u_2}{\partial x_1^2} + g\beta(T - T_{\infty}) - \frac{\sigma B_0^2}{\rho} u_2,$$

- The  $x_3$  momentum equation becomes

$$0 = -\frac{1}{\rho} \frac{\partial p}{\partial x_3} \Rightarrow \frac{\partial p}{\partial x_3} = 0 \Rightarrow p = p(x_1, x_2).$$

Hence, the momentum equations become;

$$u_{1}\frac{\partial u_{1}}{\partial x_{1}} + u_{2}\frac{\partial u_{1}}{\partial x_{2}} + u_{3}\frac{\partial u_{1}}{\partial x_{3}} = -\frac{1}{\rho}\frac{\partial p}{\partial x_{1}} + \frac{\mu}{\rho}\frac{\partial^{2} u_{1}}{\partial x_{3}^{2}} + g\beta(T - T_{\infty}) - \frac{\sigma B_{0}^{2}}{\rho}u_{1},$$

$$u_{1}\frac{\partial u_{2}}{\partial x_{1}} + u_{2}\frac{\partial u_{2}}{\partial x_{2}} + u_{3}\frac{\partial u_{2}}{\partial x_{3}} = -\frac{1}{\rho}\frac{\partial p}{\partial x_{2}} + \frac{\mu}{\rho}\frac{\partial^{2} u_{2}}{\partial x_{3}^{2}} + g\beta(T - T_{\infty}) - \frac{\sigma B_{0}^{2}}{\rho}u_{2}.$$

$$(3.2.18)$$

In a natural convection, the pressure terms the equations are ignored and the equations agree with the equations in the work of Rutto et al. (2024) as;

$$u_1 \frac{\partial u_1}{\partial x_1} + u_2 \frac{\partial u_1}{\partial x_2} + u_3 \frac{\partial u_1}{\partial x_3} = \frac{\mu}{\rho} \frac{\partial^2 u_1}{\partial x_3^2} + g\beta(T - T_{\infty}) - \frac{\sigma B_0^2}{\rho} u_1,$$

$$u_1\frac{\partial u_2}{\partial x_1} + u_2\frac{\partial u_2}{\partial x_2} + u_3\frac{\partial u_2}{\partial x_3} = \frac{\mu}{\rho}\frac{\partial^2 u_2}{\partial x_3^2} + g\beta(T-T_\infty) - \frac{\sigma B_0^2}{\rho}u_2.$$

In the equations the left-hand side represents the convective acceleration, which describes the rate of change of velocity as fluid particles move through the domain. This term accounts for the transport of momentum due to the motion of the fluid itself. On the right-hand side, there are four distinct terms that contribute to the flow. The first term is the pressure term that represents the influence of pressure on the flow. The second term represents the viscous effects, which arise due to the internal friction within the fluid caused by molecular interactions. This term accounts for the resistance to deformation and the diffusion of momentum, governed by the viscosity of the fluid. Viscous forces are responsible for determining the velocity distribution, especially in regions where shear stress is significant, that is the boundary layers. The third term accounts for buoyancy forces which arise due to temperature variations within the fluid. This is a common occurrence in natural convection flows that causes a difference in density across the fluid. The fourth term represents the body force exerted by the applied magnetic field. This effect is fundamental in magnetohydrodynamics (MHD), where the interaction between the fluid flow and the electromagnetic field governs the behaviour of conducting fluids such as plasmas, liquid metals, and ionized gases.

# III. Results Effects of Grashof Number

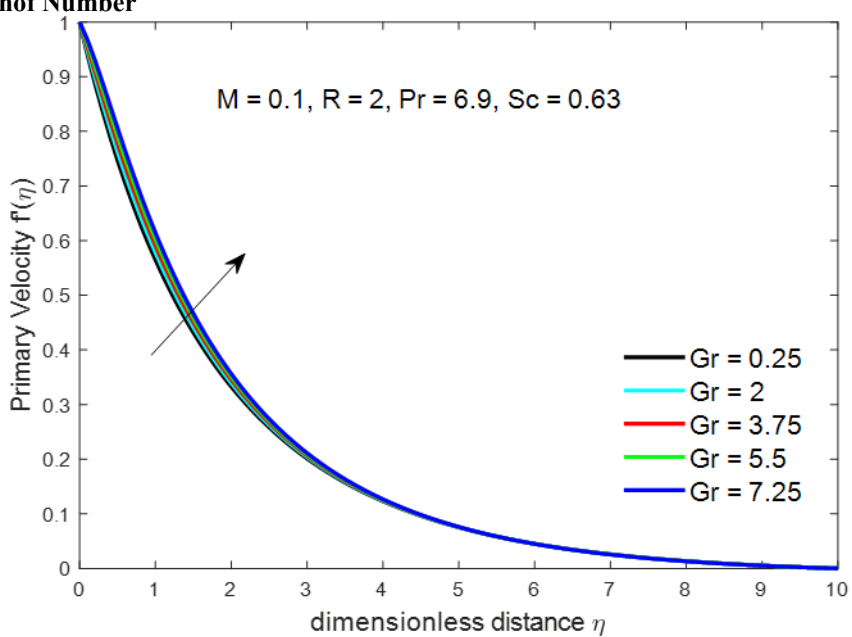


Figure 1(a): Effect of Grash of number on primary velocity

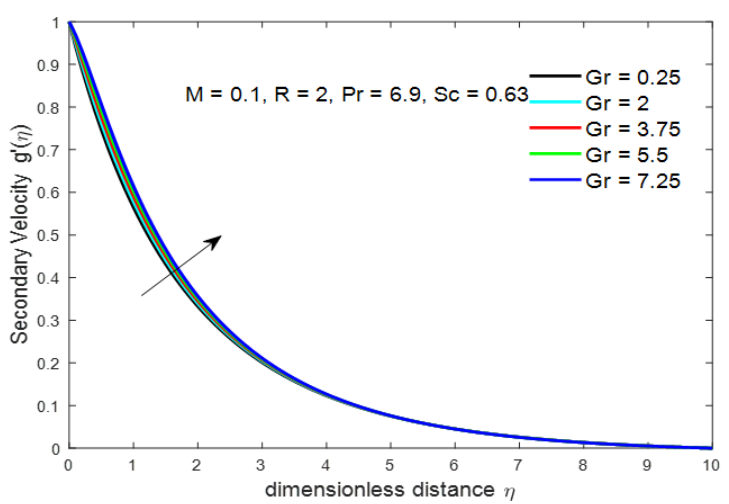


Figure 1(b): Effect of Grash of number on secondary velocity

# **Effects of Magnetic Field Parameter**

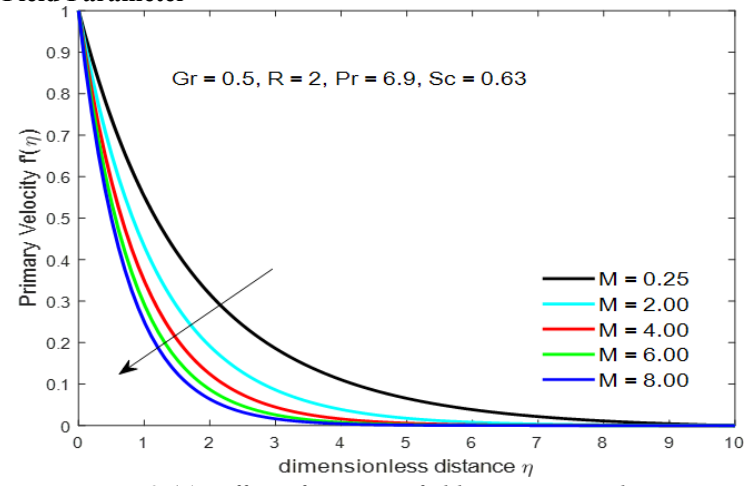


Figure 2 (a): Effect of magnetic field on primary velocity

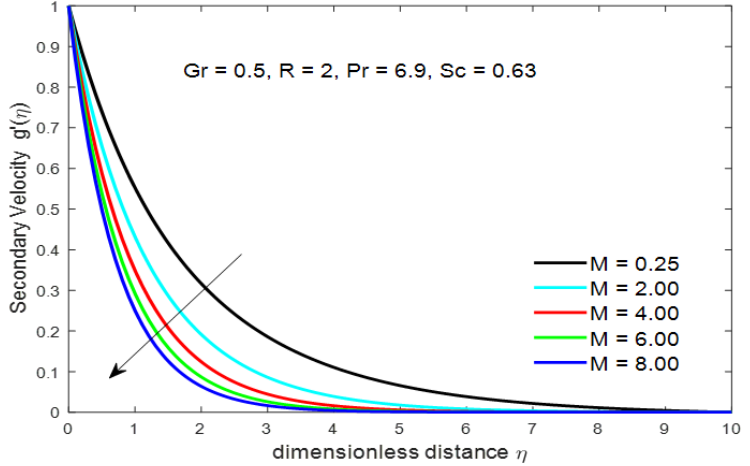


Figure 2 (b): Effect of magnetic field on secondary velocity

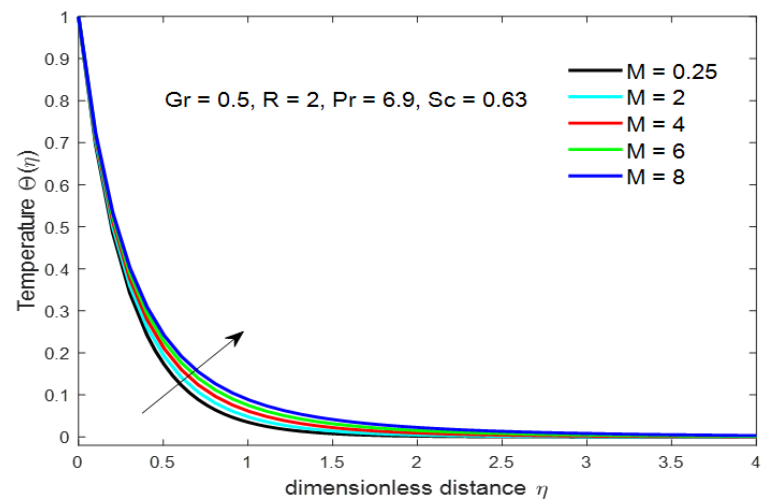


Figure 2 (c) Effect of magnetic field on temperature

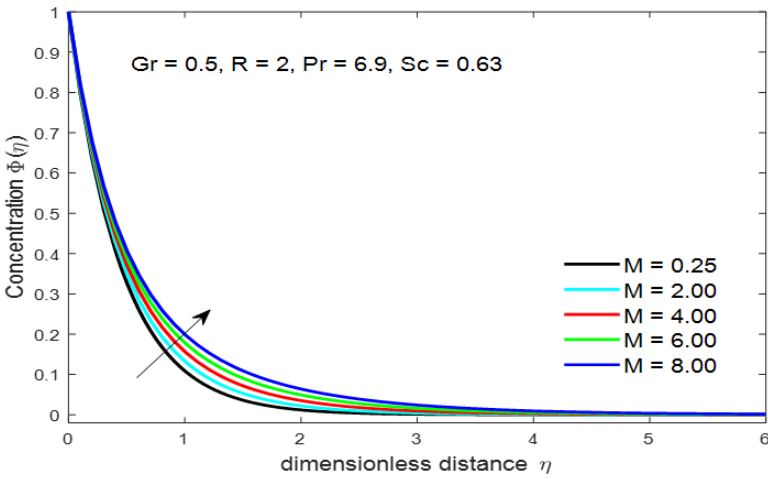


Figure 2 (d) Effect of magnetic field on concentration

# IV. Discussion

The system of dimensionless ordinary differential equations is solved over  $\eta \in [0, \eta_{\infty}]$  where  $\eta_{\infty} = 10$  to ensure convergence. The thermophysical properties of the nanofluid were incorporated into the calculations. Using water as the base fluid and silicon (IV) oxide  $(SiO_2)$  as the nanoparticles. The numerical simulations are carried out for different parameter values to study the response of velocity, temperature, and concentration distributions to the variation in the parameters. The default parameter values are

$$Gr = 0.5$$
;  $M = 0.1$ ;  $R = 2$ ;  $Pr = 6.9$ ;  $Sc = 0.63$ .

The Grashof number (Gr) represents the ratio of buoyancy forces to viscous forces in the nanofluid flow. It determines the influence of natural convection on the flow. The numerical simulations reveal that an increase in Gr leads to an enhancement in both the primary (f') and secondary (g') velocity components. These observations are primarily due to the buoyancy forces strengthening the convective transport of fluid and nanoparticles so that buoyancy forces become stronger as Gr increases, and consequently leading to an increase in the fluid velocity. The increase in velocities in both directions implies that free convection is dominant and cross-sectional flow mixing is enhanced, leading to more effective thermal energy distribution.

The numerical results indicate that increasing M leads to a reduction in both the primary velocity and secondary velocity, but it leads to increased temperature and concentration of the nanofluid. As M increases, a noticeable decline in the velocity profiles is observed, which can be attributed to the Lorenz force introduced by the magnetic field, which acts in the opposite direction to the fluid motion, thereby suppressing both primary and secondary velocities. The reduction in velocity also leads to increased viscous dissipation, which in turn influences the thermal and mass transport characteristics of the nanofluid. Also, a significant increase in temperature is observed with increasing M due to an increase in thermal boundary layer thickness arising from suppressing velocity. The concentration is also observed to increase with increasing M, probably due to the reduction in convective mixing caused by lower velocities.

. Increasing the nanoparticle volume fraction  $\phi$  thickens the viscous boundary layer and expands the region where viscosity becomes more significant. By the increase, the higher thermal conductivity of nanoparticles facilitates improved heat exchange, leading to a reduction in viscous resistance and an increase in flow acceleration. The thermal effects of  $\phi$  are significant due to the superior heat-conducting ability of nanoparticles compared to the base fluid. As  $\phi$  increases, nanoparticle interactions become more frequent, leading to greater inter-particle collisions. This reduces the mobility of individual particles, limiting their ability to diffuse freely within the base fluid. Consequently, the concentration boundary layer thickens, and nanoparticles become more localized rather than evenly distributed.

## V. Conclussion

The results show that Grashof number and nanoparticle volume fraction enhances primary and secondary velocities, magnetic field reduces both primary and secondary velocities, nanoparticle volume fractions increase temperature profile, and nanoparticle volume fractions concentration of nanoparticles decreases.

## References

- Choi, S. U., & Eastman, J. A. (1995). Enhancing Thermal Conductivity Of Fluids With Nanoparticles (No. ANL/MSD/CP-84938; CONF-951135-29). Argonne National Lab. (ANL), Argonne, IL (United States).
- [2]. Das, S. K., Choi, S. U., & Patel, H. E. (2006). Heat Transfer In Nanofluids—A Review. Heat Transfer Engineering, 27(10), 3-19.
- [3]. Elahi, F., Lotfi, M., Shafiee, M., & Daryaeipeyma, F. (2025). Investigating Thermal–Hydraulic Efficiency Of Graphene Oxide-Silica Hybrid Nanofluid Helical Coil. Heat And Mass Transfer, 61(1), 1-19.
- [4]. Murshed, S. M. S., Leong, K. C., & Yang, C. (2008). Investigations Of Thermal Conductivity And Viscosity Of Nanofluids. International Journal Of Thermal Sciences, 47(5), 560-568.
- [5]. Rutto, C. C., Chepkwony, I., & Oke, A. S. (2024). Numerical Comparison Of Cu And Al\(\_2\) O\(\_3\) Nanoparticles In An MHD Water-Based Nanofluid. Journal Of Engineering Research And Reports, 26(6), 139-146.
- [6]. Oke, A. S., Animasaun, I. L., Mutuku, W. N., Kimathi, M., Shah, N. A., & Saleem, S. (2021). Significance Of Coriolis Force, Volume Fraction, And Heat Source/Sink On The Dynamics Of Water Conveying 47 Nm Alumina Nanoparticles Over A Uniform Surface. Chinese Journal Of Physics, 71, 716-727.
- [7]. Zhang, L., Zhang, A., Jing, Y., Qu, P., & Wu, Z. (2021). Effect Of Particle Size On The Heat Transfer Performance Of Sio2–Water Nanofluids. The Journal Of Physical Chemistry C, 125(24), 13590-13600.
- [8] Juma, B. A., Oke, A. S., Ariwayo, A. G., & Ouru, O. J. (2022). Theoretical Analysis Of MHD Williamson Flow Across A Rotating Inclined Surface. Applied Mathematics And Computational Intelligence (AMCI), 11(1), 133-145.
- [9]. Das, S. K., Choi, S. U., & Patel, H. E. (2006). Heat Transfer In Nanofluids—A Review. Heat Transfer Engineering, 27(10), 3-19.